



Journal Name

COMMUNICATION

Synthesis and reactivity of rare-earth metal phosphaehtynolates

 Sebastian Bestgen,^a Qien Chen,^a Nicholas H. Rees,^a and Jose M. Goicoechea^{a*}

 Received 00th January 20xx,
 Accepted 00th January 20xx

DOI: 10.1039/x0xx00000x

www.rsc.org/

Over the course of the last six years, research on the synthesis and reactivity of molecular metal phosphaketenes (M–PCO) has gained increasing attention. However, lanthanide complexes of the heavier group 15 cyanate analogue PCO[−] have not been investigated so far. Herein we present exemplar studies on the nature and reactivity of rare-earth phosphaehtynolato-complexes using three characteristic representatives of the lanthanide metals: Y, Nd and Sm. Our investigations comprise both +2 and +3 redox states, one defined amidinate-based ligand set, as well as novel reaction pathways in the presence of the sequestering agents 18-crown-6 and 2,2,2-crypt.

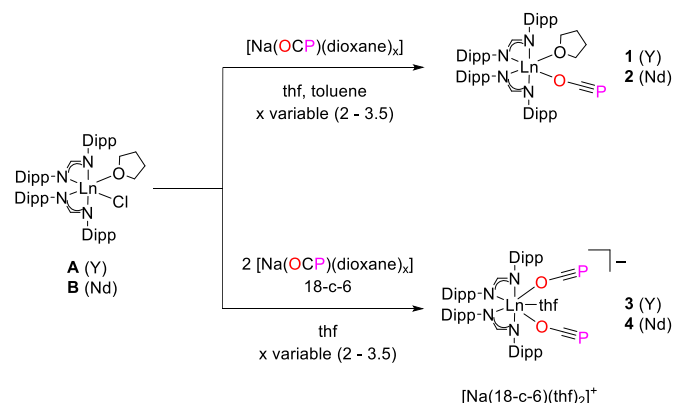
The 2-phosphaehtynolate anion PCO[−] is the heavier analogue of the well-known cyanate ion NCO[−]. Although it was isolated in 1992 by Becker *et al.* as [Li(DME)₂][PCO] (DME = dimethoxyethane),¹ its chemistry remained unexplored until more reliable and high-yielding synthetic procedures were reported.^{2–5} Since 2014, many efforts have been made to explore the chemistry of this ion and it has been shown to be a convenient precursor to a variety of novel compounds.^{6–11} The accessibility of PCO[−] salts has allowed for the investigation of molecules such as HPCO (the heavy analogue of isocyanic acid),¹² and also stimulated research on heavier derivatives such as the 2-phosphathioethynolate ion, PCS[−], or the 2-arsaehtynolate ion, AsCO[−].^{13–15} For the PCO[−] anion, two resonance structures best illustrate the bonding situation, which lies between a phosphaketinide [−P=C=O] and a phosphaehtynolate [P≡C–O[−]], being slightly dominated by the latter (40.2% vs. 51.7%).¹⁶ Consequently, the 2-phosphaehtynolate anion is ambiphilic and able to bind to Lewis acids either through its phosphorus or oxygen atom, which significantly affects its bonding and spectroscopic properties and subsequent reactivity. Molecular examples of the phosphaketinyl bonding mode [LA–PCO] (LA = Lewis Acid)

vastly outnumber the phosphaehtynolato bonding mode [LA–OCP], and are often found to facilitate consecutive reactions via decarbonylation pathways. Structurally authenticated phosphaehtynolato compounds are fewer in number and have only been realized for U, Th, Sc, Ca and Mg.^{17–21} Very recently, we demonstrated that the phosphaehtynolato bonding mode is also accessible for boranes which allowed for dimerization and photoinduced decarbonylation processes.²² Given our interest in the coordination behaviour of the PCO[−] ion and that lanthanide-phosphaehtynolate complexes have not been reported so far, we reasoned that many stable phosphaehtynolato complexes should be accessible by exploiting their electropositive and strongly oxophilic character. Since the rare-earth metal series comprises a family of seventeen elements, we decided to investigate three representative elements, which we believe cover and reflect their properties and reactivity best: 1) Yttrium, as a diamagnetic and NMR-active species to monitor and analyse reactions in solution; 2) Neodymium, as a typical paramagnetic, coloured trivalent lanthanide; and 3) Samarium, as the metal provides access to the +2 and +3 redox states.

Additionally, we aimed to utilize a single ligand system, which would preferably only act as spectator ligand and be suitable for all rare-earth metals, in order to assure comparability and exclude significant ligand effects. Thus, we chose the bulky formamidinate ligand DippForm (DippForm = *N,N'*-bis(2,6-diisopropylphenyl)-formamidinate), which has successfully been used in organometallic chemistry and been found to stabilize rare-earth metal complexes in different oxidation states.^{23–30} The amidinate rare-earth metal complexes [(DippForm)₂Ln(Cl)_x(thf)_y] (Ln = Y (**A**), Nd (**B**), Sm (**C**); *x*, *y* = 1 for Y, Nd; *x* = 0, *y* = 2 for Sm; thf = tetrahydrofuran) were obtained via salt metathesis from KDippForm and LnCl₃ (Y, Nd) or SmI₂(thf)₂ in a 2:1 ratio. It is worth noting that KDippForm and Dippform–Ln complexes were reported previously by Deacon, Junk and co-workers albeit via different synthetic methods.^{23, 31–33} For the trivalent complexes **A** and **B**, one Cl[−] anion is still bonded to the metal, which should enable subsequent salt metathesis reactions with [Na(OCP)(dioxane)_x]

^a Department of Chemistry, University of Oxford, Chemistry Research Laboratory, 12 Mansfield Road, OX1 3TA Oxford, United Kingdom.
 E-mail: jose.goicoechea@chem.ox.ac.uk
 Electronic Supplementary Information (ESI) available: Experimental, analytical and crystallographic data. See DOI: 10.1039/x0xx00000x

($x = 2\text{--}3.5$) eliminating NaCl. Indeed, the reaction of **A** or **B** with $[\text{Na}(\text{OCP})(\text{dioxane})_x]$ in thf cleanly led to the isolation of the phosphaehtynolato species $[(\text{DippForm})_2\text{Ln}(\text{OCP})(\text{thf})]$ ($\text{Ln} = \text{Y}$ (**1**) and $\text{Ln} = \text{Nd}$ (**2**)) in fair yields (Scheme 1).



Scheme 1 Synthesis of the rare-earth phosphaehtynolates $[(\text{DippForm})_2\text{Ln}(\text{OCP})(\text{thf})]$ ($\text{Ln} = \text{Y}$ (**1**), Nd (**2**)) and bis-phosphaehtynolates $[\text{Na}(18\text{-crown-6})(\text{thf})_2][(\text{DippForm})_2\text{Ln}(\text{OCP})_2(\text{thf})]$ ($\text{Ln} = \text{Y}$ (**3**), Nd (**4**)).

Both complexes feature enhanced solubility compared to the starting materials and **2** represents the first lanthanide-phosphaehtynolate synthesized to date. The synthesis of a rare-earth metal phosphaehtynolate was unambiguously proven by $^{31}\text{P}\{^1\text{H}\}$ NMR spectroscopy. For **1**, a sharp singlet is observed at -346.9 ppm, which is significantly downfield-shifted compared to $[\text{Na}(\text{OCP})(\text{dioxane})_x]$ (-392 ppm) or $[\text{Mg}(\text{OCP})_2(\text{thf})_4]$ (-367.9 ppm) and similar to the ^{31}P NMR shift found for $[(\text{NacNac})\text{Sc}(\text{OAr})(\text{OCP})(\text{thf})]$ ($\text{NacNac} = [\text{ArNC}(\text{CH}_3)]_2\text{CH}$; $\text{Ar} = 2,6\text{-iPr}_2\text{C}_6\text{H}_3$), -343.5 ppm.^{19, 20} Signal splitting due to $^3J_{\text{Y-P}}$ coupling was not observed within the boundaries of resolution. As $^2J_{\text{Y-P}}$ coupling constants of Y-P compounds can already be quite small (e.g. $^2J_{\text{Y-P}} = 6.5$ Hz and $^4J_{\text{Y-P}} < 1$ Hz in $\text{Y}\{[\text{Ph}_2\text{P}(\text{O})]_3\text{C}\}$),³⁴ we assume the longer range $^3J_{\text{Y-P}}$ coupling constant in **1** to be negligible. In the $^{13}\text{C}\{^1\text{H}\}$ spectrum, the carbon resonance for the OCP^- unit is split into a doublet of doublets with $^1J_{\text{P-C}} = 7.3$ Hz and $^2J_{\text{Y-C}} = 4.3$ Hz indicating an yttrium-bound phosphaehtynolato ligand rather than a phosphaketene, the P–C coupling constant of which would be larger (Figure 1). Additionally, $^1\text{H}\{^{89}\text{Y}\}$ HMQC and $^{89}\text{Y}\{^1\text{H}\}$ INEPT spectra were recorded monitoring NCHN coupling to Y, and the nuclear resonance of ^{89}Y itself (Figure 1).

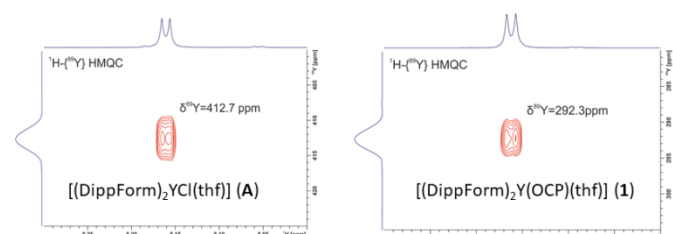


Figure 1 $^1\text{H}\{^{89}\text{Y}\}$ HMQC spectra of $[(\text{DippForm})_2\text{YCl}(\text{thf})]$ **A** (left) and $[(\text{DippForm})_2\text{Y}(\text{OCP})(\text{thf})]$ **1** (right).

Whereas for **A**, a cross peak is observed at $\delta(^{89}\text{Y}) = 412$ ppm / $\delta(^1\text{H}) = 8.17$ ppm with $^3J_{\text{Y-H}} = 3.6$ Hz, the yttrium resonance in **1** is shifted upfield and located at $\delta(^{89}\text{Y}) = 292$ ppm / $\delta(^1\text{H}) = 8.12$ ppm with $^3J_{\text{Y-H}} = 3.9$ Hz and thus significantly shifted upon ligand exchange from Cl^- to OCP^- . $^{89}\text{Y}\{^1\text{H}\}$ INEPT spectra confirm these findings, showing a singlet at 292 ppm with again no visible ^{31}P -coupling (See ESI).

NMR investigations of **2** reveal a paramagnetically broadened and unstructured ^1H spectrum. However, a sharp singlet is observed in the $^{31}\text{P}\{^1\text{H}\}$ NMR spectrum at -292.2 ppm, which is clearly shifted downfield and in a comparable range to the paramagnetic U(IV) complex $[(\text{amid})_3\text{U}(\text{OCP})]$ (-285 ppm, amid = N,N' -bis-(trimethylsilyl)benzamidinate).¹⁷ IR spectra of **1** and **2** feature bands at 1691 and at 1684 cm^{-1} respectively, which are attributed to the ν_1 “antisymmetric” stretching vibrational mode of the OCP^- ligand. Final proof for the synthesis of **1** and **2** was achieved via X-ray diffraction experiments. Both compounds crystallize in the triclinic space group $P\bar{1}$, however in the case of **2**, three crystallographically independent molecules were found in the asymmetric unit (Figure 2 for Y, for Nd: See ESI).

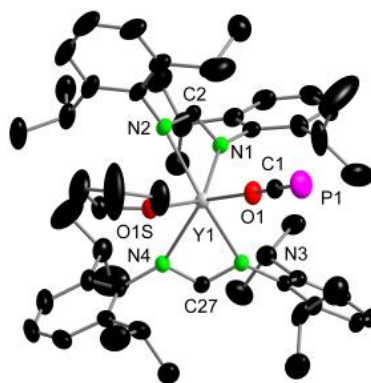


Figure 2 Molecular structure of $[(\text{DippForm})_2\text{Y}(\text{OCP})(\text{thf})]$ (**1**) in the solid state. Hydrogen atoms and solvent molecules are omitted for clarity.

The Y1–O1 distance (2.1562(12) Å) is in the range for yttrium alkoxides and elongated compared to $[(\text{NacNac})\text{Sc}(\text{OAr})(\text{OCP})(\text{thf})]$ ($\text{Sc1}–\text{O1}$ 2.032 Å) due to its larger ionic radius.¹⁹ Bonding parameters within the OCP^- unit are P1–C1 1.559(2) and C1–O1 1.250(2) Å with a linear angle of O1–C1–P1 178.5(2)°. The 2-phosphaehtynolato ligand binds to Y in an almost linear fashion (Y1–O1–C1 167.74(13)°), and given that bond distances are very similar to $[\text{Na}(\text{OCP})(\text{dioxane})_{2.5}]$, a phosphaehtynolato-type structure instead of a phosphaketene structure with a $\text{P}\equiv\text{C}$ triple bond and a C–O single bond is realized. This conclusion is also valid for the neodymium complex **2**, however bonding parameters vary for the three independent molecules and thus illustrate the influence of packing effects on phosphaehtynolato compounds. Nd1–O1 bond lengths are between 2.224(3) Å and 2.349(5) Å and vary more than the P–C (1.557(6)–1.595(14) Å) or C–O bond lengths (1.192(14)–1.252(6) Å). Most interestingly, Nd–O–C angles vary significantly and are between 117.6(5)° and 166.5(4)° thus switching between an angled and a quasi-linear coordination mode while maintaining

linearity of the OCP unit (O–C–P 177.3(5)–178.9(6)°). It is worth noting that for species with more acute Nd–O–C angles, the P≡C bonds are longer and the C–O bond shorter.

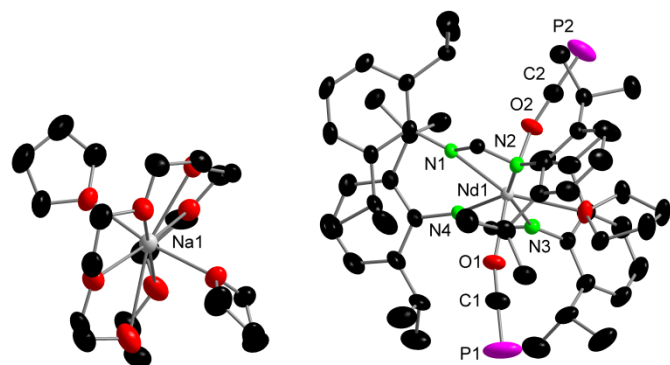
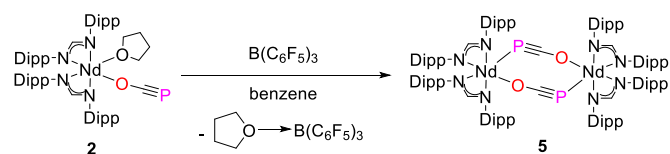


Figure 3 Molecular structure of $[\text{Na}(\text{18-crown-6})(\text{thf})_2][(\text{DippForm})_2\text{Nd}(\text{OCp})_2(\text{thf})]$ (**4**) in the solid state. Hydrogen atoms and solvent molecules are omitted for clarity.

Thus, a higher contribution of the phosphaketenide-type structure accompanies a bent coordination mode. During our attempts to synthesize **1** and **2**, we observed NMR resonances indicative of the formation of different complexes, when using an excess of $[\text{Na}(\text{OCp})(\text{dioxane})_x]$. As the formation of -ate complexes was a likely explanation, we conducted a targeted synthesis of ionic bis-phosphaethynolate complexes of Y and Nd, by using two equivalents of $[\text{Na}(\text{OCp})(\text{dioxane})_x]$ in the presence of the sequestering agent 18-crown-6. Indeed, the bis-phosphaethynolate complexes $[\text{Na}(\text{18-crown-6})(\text{thf})_2][(\text{DippForm})_2\text{Ln}(\text{OCp})_2(\text{thf})]$ (**3**: Y; **4**: Nd) were obtained as crystalline materials and represent rare examples of bis-OCp-complexes (Scheme 1, Figure 3 for Nd (**4**)). Both metals are heptacoordinate with the two OCp-ligands in *trans*-positions to each other (O1–Y1–O2 173.06(7), O1–Nd1–O2 170.96(6)). For **3**, an even more upfield shifted resonance at 147.3 ppm is observed in the $^{89}\text{Y}\{^1\text{H}\}$ INEPT spectrum. The complex shows hindered rotation of the Dipp moieties, as proven by variable temperature (VT) NMR spectroscopy (See SI). For paramagnetic **4**, a very similar shift compared to **2** at –289.7 ppm is seen in the $^{31}\text{P}\{^1\text{H}\}$ NMR spectrum.

With our phosphaeethynolato-complexes in hand, we next aimed to investigate their reactivity. As OCp[–] is an ambiphilic anion, we wondered whether bridging coordination modes could be achieved. We therefore treated **1** and **2** with the strong Lewis acid $\text{B}(\text{C}_6\text{F}_5)_3$ and monitored the reactions by NMR spectroscopy (Scheme 2). For **1**, no significant changes were observed in the $^{31}\text{P}\{^1\text{H}\}$ spectra indicating that no Y–OCp→ $\text{B}(\text{C}_6\text{F}_5)_3$ Lewis adduct formed or rearrangement processes took place.



Scheme 2 Synthesis of the dimeric species **5** upon thf abstraction with $\text{B}(\text{C}_6\text{F}_5)_3$.

In contrast, the same reaction for **2**, which features a larger metal ion, led to the formation of a crystalline product from benzene. Thus, X-ray analysis was performed and revealed the dimeric species $[(\text{DippForm})_2\text{Nd}(\mu_2\text{:}\kappa^1\text{O},\kappa^2\text{P-OCp})_2]$ (**5**) (Figure 4).

Each Nd ion in **5** is coordinated by two DippForm ligands and two OCp/PCO moieties, which act as bridging $\mu_2\text{:}\kappa^1\text{O},\kappa^2\text{P-OCp}$ ligands between the metal centres. Upon reaction with the strong Lewis acidic borane, decomplexation of the parent metal complex occurs, and Nd-bound thf is removed from the coordination sphere to form the Lewis adduct $(\text{thf})\text{B}(\text{C}_6\text{F}_5)_3$. Thus, the central part of the structure is a planar rectangular $[\text{Nd}(\text{OCp})]_2$ unit featuring short Nd–O (2.352(3) Å) and long Nd–P (3.058(2) Å) bonds. For the OCp[–] moiety, the bond lengths (C–O 1.234(5) Å and P–C 1.582(4) Å) and the O–C–P angle (176.0(4)°) remain essentially unaffected and compare favourably to those in **2**. An almost linear coordination for Nd–OCp (C1–O1–Nd1 173.0(3)°) and direct coordination of a phosphaealkyne to an f-element is observed. Complex **5** is largely insoluble in benzene/toluene, and consequently, NMR studies were conducted in $\text{thf-}d_8$. In the $^{31}\text{P}\{^1\text{H}\}$ NMR spectrum, a sharp singlet appears at –278.1 ppm, which is slightly shifted downfield compared with **2** and **4**.

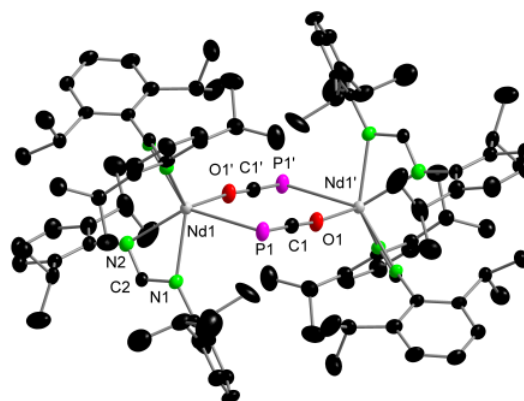
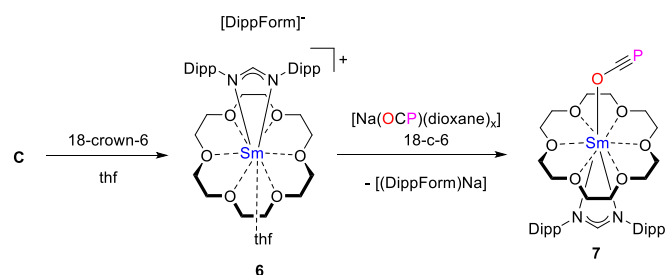


Figure 4 Molecular structure of $[(\text{DippForm})_2\text{Nd}(\mu_2\text{:}\kappa^1\text{O},\kappa^2\text{P-OCp})_2]$ (**5**) in the solid state. Hydrogen atoms and solvent molecules (benzene) are omitted for clarity.

Based on these results, we were prompted to investigate the reactivity of the divalent lanthanide complex $[(\text{DippForm})_2\text{Sm}(\text{thf})_2]$ (**C**) with $[\text{Na}(\text{OCp})(\text{dioxane})_x]$. An equimolar mixture of $[(\text{DippForm})_2\text{Sm}(\text{thf})_2]$ and $[\text{Na}(\text{OCp})(\text{dioxane})_x]$ was dissolved in $\text{thf-}d_8$ and monitored by NMR spectroscopy. A sharp singlet is seen in the high field region at –367.1 ppm, suggesting the formation of an ate-type complex $[\text{Na}(\text{solv})_x][(\text{DippForm})_2\text{Sm}(\text{OCp})(\text{thf})]$, which we could not crystallize. Addition of 18-crown-6 to **C** in the coordinating solvent thf cleanly led to the formation of a divalent cationic complex $[(\text{DippForm})\text{Sm}(\text{18-crown-6})(\text{thf})][\text{DippForm}]$ (**6**), in which one amidinate ligand is replaced by the hexadentate crown ether (Scheme 3, Figure 5 left). Rather long Sm–N bond lengths of Sm1–N1 2.707(4) Å and Sm1–N2 2.649(4) Å support the divalent oxidation state, as significantly shorter Sm–N bond lengths are generally found for trivalent species.^{26, 27}



Scheme 3 Synthesis of the divalent Sm(II) intermediate **6** and OCP[−] complex **7** (**C** is [(DippForm)₂Sm(thf)₂]).

Surprisingly, a bidentate anionic ligand was found to be replaceable by a neutral sequestering agent, leading to a rare cationic, divalent lanthanide complex. This is reminiscent of the displacement of ionic η⁵-1,3-C₅H₃(SiMe₃)₂ (Cp[−]) ligands in solvent-free [LnCp[−]]₂ (Ln = Yb, Sm) by 18-c-6, which has been observed by Lappert, leading to the first cationic Ln(II) complex.³⁵ In **6**, the coordinating thf molecule should be easily replaceable by other ligands. To probe this, we subsequently added [Na(OCP)(dioxane)_x] to **6**, which lead to the elimination of [(DippForm)Na(thf)_x] and the formation of the phosphaehtynolate complex [(DippForm)Sm(OCP)(18-crown-6)] (**7**) (Scheme 3). Single crystals suitable for structural analysis were obtained (Figure 5 right). In ³¹P{¹H} NMR spectra, a singlet is observed at −391.7 ppm. The antisymmetric stretching mode of the OCP[−] ligand is seen at 1758 cm^{−1}. Due to the larger ionic radius of Sm(II), the Sm1–O1 bond (2.610(3) Å) is elongated compared with e.g. **1** and **2**. Rather long Sm–N distances (2.642(3) Å and 2.655(3) Å) again substantiate the oxidation state to be +2.

In order to investigate whether the addition of other sequestering agents was also of preparative use, we aimed to synthesize a divalent bis-phosphaehtynolate Sm complex by using 2,2,2-crypt. Indeed, the addition of 2,2,2-crypt to **C** quantitatively leads to the cationic species [(DippForm)Sm(2,2,2-crypt)][DippForm] (**8**), which directly crystallizes from thf (Scheme 4 and Figure 6, left).

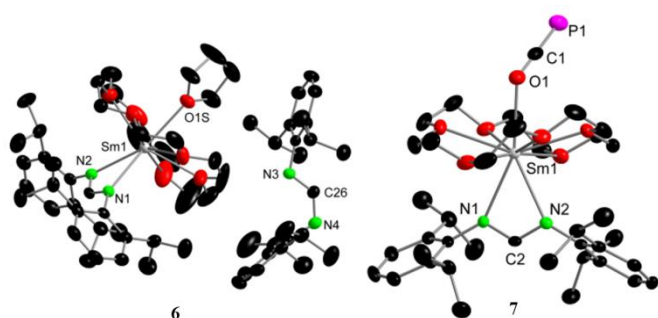
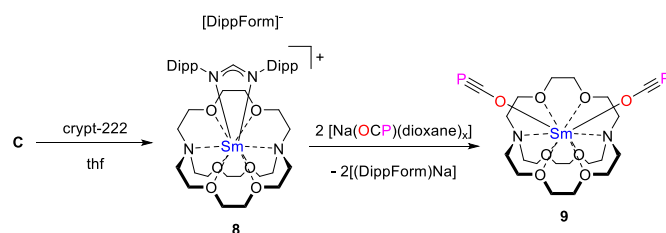


Figure 5 Molecular structure of **6** (left) and **7** (right) in the solid state. Hydrogen atoms are omitted.



Scheme 4 Synthesis of the divalent Sm(II) intermediate **8** and OCP[−] complex **9** (**C** is [(DippForm)₂Sm(thf)₂]).

In **8**, a Sm²⁺-in-crypt complex is seen, in which the Sm centre is loosely bound to one amidinate ligand (as indicated by the significantly elongated Sm–N distances of Sm1–N1 2.790(3) and Sm1–N2 2.799(3) Å), whereas the second one remains uncoordinated.

These very rare Ln²⁺-in-crypt complexes have only been observed very recently by Evans and co-workers, and indeed seem to be accessible by exchanging ionic ligands with neutral chelating agents.³⁶ Noteworthy, reductive cleavage of crypt C–O bonds by Sm²⁺, as seen by Evans, was not observed in our case. Subsequently, we treated **8** with two equivalents of [Na(OCP)(dioxane)_x], which led to the rapid formation of a red crystalline precipitate, [(2,2,2-crypt)Sm(OCP)₂] (**9**) (Figure 6, right). Indeed, both amidinate ligands were eliminated as [(DippForm)Na(thf)_x], and the neutral Sm-bis-phosphaehtynolate complex **9** was formed. Consequently, the combination of sequestering agents and lanthanide amidinates can be used for novel ligand exchange reactions. To the best of our knowledge, **9** is the first divalent, charge-neutral coordination compound of the lanthanides and 2,2,2-crypt. Formally, Sm(OCP)₂ is encapsulated by the cryptand leading to tenfold coordination. Both OCP[−] ligands are adjacent to each other with O1–Sm1–O2 134.3(2)°, and feature similar P–C and C–O bond lengths as **7**. The first neutral non-s-block diphosphaehtynolate complex **9** is perfectly stable under inert conditions, despite the strong reduction potential of Sm(II). In summary, we have explored the synthesis and reactivity of rare-earth-metal amidinate complexes towards the heavier cyanate analogue PCO[−]. Their formation and coordination behaviour was studied, including heteronuclear ⁸⁹Y NMR spectroscopy. For the highly oxophilic rare-earth elements, the phosphaehtynolate bonding mode is observed and a variety of such complexes should be accessible by using different ligand sets.

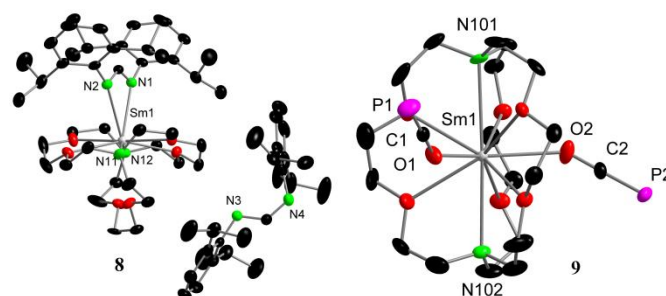


Figure 6 Molecular structure of **8** (left) and **9** (right) in the solid state. Hydrogen atoms are omitted.

A series of mono- and bis-phosphaethynolate complexes in different oxidation states was prepared, revealing an unprecedented bridging mode of PCO^- within the first lanthanide phosphaaalkyne. For $[(\text{DippForm})_2\text{Sm}(\text{thf})_2]$, the usage of sequestering agents led to the displacement of the anionic amidinate ligands providing access to rare ionic $\text{Sm}(\text{II})$ intermediates. By exploiting the elimination of $[(\text{DippForm})\text{Na}(\text{thf})_x]$ in the presence of 18-crown-6 or 2,2,2-crypt, the so obtained species are expected to have a rich chemistry with respect to reductive activation of small molecules and/or novel coordination compounds, that are otherwise not accessible.

Experimental details

n-Pentane, *n*-hexane (hex; Sigma-Aldrich, HPLC grade), benzene and toluene (Sigma-Aldrich; HPLC grade) were purified using an MBraun SPS-800 solvent system. Tetrahydrofuran (thf; Sigma-Aldrich, HPLC grade) was distilled over sodium metal/benzophenone. All dry solvents were stored under argon in gas-tight ampoules. Additionally, *n*-pentane, *n*-hexane and thf were stored over activated 3 Å molecular sieves. thf- d_8 (Sigma-Aldrich, 99.5%) was dried over CaH_2 and vacuum distilled before use. C_6D_6 was stored over activated 3 Å molecular sieves and degassed prior to use. Potassium bis(trimethylsilyl)amide (KHMDs) was purchased from Sigma Aldrich (95 %) and used as received. Anhydrous YCl_3 and NdCl_3 were purchased from Strem chemicals and used as received. Sm metal was obtained from smart-elements® GmbH (Austria). $[\text{Na}(\text{OCP})(\text{dioxane})_x]$ ($x = 3.42, 2$ or 0.3) was prepared according to literature procedures.⁵ The dioxane content was determined by $^{31}\text{P}\{^1\text{H}\}$ NMR spectroscopy using PPh_3 as internal standard. $\text{B}(\text{C}_6\text{F}_5)_3$ was prepared according to literature procedures.³⁷ *N*, *N'*-bis(2,6-diisopropylphenyl)formamidine (DippFormH),³⁸ $\text{SmI}_2(\text{thf})_2$,³⁹ and $[(\text{DippForm})_2\text{Sm}(\text{thf})_2]$ ^{23, 27} were prepared according to literature procedures. DippFormK was reported previously using a slightly different procedure.³³

Compound syntheses

Synthesis of $[(\text{DippForm})_2\text{YCl}(\text{thf})]$ (A)
 $[(\text{DippForm})\text{K}]$ (1.275 g, 3.17 mmol, 2.00 eq.) and anhydrous YCl_3 (309 mg, 1.58 mmol, 1.00 eq.) were added to a Schlenk tube and dissolved in thf (20 mL). After stirring at 50 - 60 °C overnight, the solvent was removed under vacuum and the residue was extracted with toluene (2 x 10 mL). After filtration using a filter cannula, a clear colorless solution was obtained, which was concentrated until incipient precipitation occurred. Colorless crystals suitable for single crystal X-ray diffraction were obtained from a saturated toluene solution at room temperature. Yield: 765 mg (52 %, single crystals). ^1H NMR (500.3 MHz, C_6D_6): δ [ppm] = 0.75 (m, 4H, OCH_2CH_2 (thf)), 1.19 (d, $^3J_{\text{H-H}} = 6.8$ Hz, 48H, CHMe_2), 3.66 (m, overlapping, 4H, OCH_2 (thf)), 7.02 - 7.10 (m, 12H, CH), 8.17 (d, $^3J_{\text{H-Y}} = 3.6$ Hz, 2H, NCHN). $^{13}\text{C}\{^1\text{H}\}$ NMR (125.8 MHz, C_6D_6): δ [ppm] = 23.4 (CHMe_2), 25.1 (OCH_2CH_2 (thf)), 26.8 (CHMe_2), 28.5 (CHMe_2), 71.4 (OCH_2 (thf)), 123.9 (m-C), 125.3 (p-C), 143.9 (o-C), 145.1

(ipso-C), 171.6 (d, $^2J_{\text{C-Y}} = 3.3$ Hz, NCHN). $^{89}\text{Y}\{^1\text{H}\}$ INEPT NMR (19.6 MHz, C_6D_6): δ [ppm] = 412.7. $^1\text{H}\{-^{89}\text{Y}\}$ HMQC NMR ((400.2 MHz / 19.6 MHz), C_6D_6): δ [ppm] = 8.17 / 412.7. IR (Nujol, cm^{-1}): 1668 (w), 1593 (w), 1525 (s), 1460 (s), 1378 (s), 1319 (w), 1276 (s), 1261 (m), 1194 (w), 1097 (m), 1057 (m), 1045 (m), 1017 (m), 945 (w), 862 (w), 801 (m), 775 (w), 758 (w), 722 (w), 672 (w).

Synthesis of $[(\text{DippForm})_2\text{NdCl}(\text{thf})]$ (B)
 $[(\text{DippForm})\text{K}]$ (1.56 g, 3.87 mmol, 2.00 eq.) and anhydrous NdCl_3 (486 mg, 1.93 mmol, 1.00 eq.) were added to a Schlenk tube and dissolved in thf (20 mL). After stirring at 50 - 60 °C overnight, the solvent was removed under vacuum and the residue was extracted with toluene (2 x 10 mL). After filtration using a filter cannula, a clear blueish solution was obtained, which was concentrated until incipient precipitation occurred. The suspension was heated until a clear solution was obtained. Overnight, a small amount of microcrystalline precipitate formed, which was separated from the mother liquor by filtration and discarded. Storing the so obtained solution at ambient temperature afforded large blueish-purple crystals within 48 hours, which were isolated and dried under vacuum. A second crop of crystals was obtained by further concentrating the mother liquor and storage for a week. Yield: 920 mg (50 %, single crystals). ^1H NMR (400.2 MHz, C_6D_6): δ [ppm] = -3.14, -1.34, 2.32, 7.66, 9.04, 25.64. Due to the paramagnetic nature of 1, only broad and unstructured resonances were observed. IR (Nujol, cm^{-1}): 1665 (m), 1592 (w), 1523 (s), 1362 (m), 1316 (m), 1279 (s), 1261 (m), 1234 (w), 1191 (m), 1177 (m), 1160 (w), 1108 (m), 1097 (m), 1056 (w), 1043 (w), 1016 (m), 942 (w), 934 (w), 863 (w), 800 (m), 775 (m), 757 (m), 757 (m), 722 (m). Elemental analysis calcd (%) for $[\text{C}_{54}\text{H}_{78}\text{ClN}_4\text{NdO}]$ (978.94 g/mol): C 66.25, H 8.03, N 5.72; found C 66.18, H 8.09, N 5.42.

Synthesis of $[(\text{DippForm})_2\text{Y}(\text{OCP})((\text{thf}))]$ (1)
The complex $[(\text{DippForm})_2\text{YCl}(\text{thf})]$ (A) (300 mg, 0.33 mmol, 1.00 eq.) and $[\text{Na}(\text{OCP})(\text{dioxane})_{3.42}]$ (130 mg, 0.33 mmol, 1.00 eq.) were dissolved in thf (10 mL) and stirred overnight. The solvent was then removed under vacuum and the residue was extracted with toluene (10 mL) and filtered. Upon concentration of the organic phase, colorless crystals formed after 2 days and were separated from the mother liquor by decantation. Yield: 136 mg (44 %, single crystals). ^1H NMR (500.3 MHz, C_6D_6): δ [ppm] = 0.82 (m, 4H, CH_2 , thf), 1.21 (bs, 48H, CH_3), 3.46 (hept, $^3J_{\text{H-H}} = 6.9$ Hz, 8H, $\text{CH}(\text{CH}_3)_2$), 3.74 (m, 4H, CH_2 , thf), 7.00 - 7.08 (m, 12H, CH), 8.12 (d, $^3J_{\text{H-Y}} = 3.9$ Hz, 2H, NCHN). $^{13}\text{C}\{^1\text{H}\}$ NMR (125.8 MHz, C_6D_6): δ [ppm] = 23.8 (CHMe_2), 25.1 (OCH_2CH_2 (thf)), 26.7 (CHMe_2), 28.9 (CHMe_2), 71.0 (OCH_2 (thf)), 123.8 (m-C), 125.5 (p-C), 143.6 (o-C), 144.5 (d, $^2J_{\text{C-Y}} = 1.3$ Hz, ipso-C), 156.0 (dd, $^1J_{\text{C-P}} = 7.3$ Hz, $^2J_{\text{C-Y}} = 4.4$ Hz, OCP), 172.1 (d, $^2J_{\text{C-Y}} = 3.4$ Hz, NCHN). $^{31}\text{P}\{^1\text{H}\}$ NMR (162.0 MHz, C_6D_6): δ [ppm] = -346.9. $^{89}\text{Y}\{^1\text{H}\}$ INEPT NMR (19.6 MHz, C_6D_6): δ [ppm] = 292.3 (s). $^1\text{H}\{-^{89}\text{Y}\}$ HMQC NMR ((400.2 MHz / 19.6 MHz), C_6D_6): δ [ppm] = 8.12 / 292.3. IR (Nujol, cm^{-1}): 1691 (OCP), 1668 (w), 1520 (m), 1461 (s), 1377 (s), 1316 (w), 1272 (m), 1191 (w), 1098 (m), 1056 (b), 923 (w), 865 (w), 801 (w), 757 (w), 721 (w), 667 (w). Elemental analysis calcd (%) for

[C₅₅H₇₈N₄O₂PY] (947.13 g/mol): C 69.75, H 8.30, N 5.92; found C 69.25, H 8.32, N 5.72.

Synthesis of [(DippForm)₂Nd(OCp)(thf)] (2)

The complex [(DippForm)₂NdCl(thf)] (**B**) (164 mg, 0.16 mmol, 1.00 eq.) and [Na(OCp)(dioxane)_{3.42}] (75 mg, 0.19 mmol, 1.20 eq.) were dissolved in thf (10 mL) and stirred overnight at 50 °C. The solvent was then removed under vacuum and the residue was extracted with toluene (10 mL) and filtered. Upon concentration of the organic phase, colorless crystals formed after 2 days and were separated from the mother liquor by decantation. Yield: 90 mg (57 %, single crystals). ¹H NMR (400.2 MHz, C₆D₆): δ [ppm] = −3.16, −2.37, 1.15, 1.78, 2.28, 6.08, 7.52, 8.88, 14.76, 24.32. Due to the paramagnetic nature of **4**, only broad and unstructured resonances were observed. ³¹P{¹H} NMR (162.0 MHz, C₆D₆): δ [ppm] = −292.2. IR (Nujol, cm^{−1}): 1685 (w, OCp), 1667 (m), 1591 (w), 1363 (m), 1316 (w), 1278 (m), 1260 (s), 1234 (w), 1189 (w), 1095 (br), 1019 (br), 943 (w), 862 (w), 800 (s), 757 (m), 721 (w). Elemental analysis calcd (%) for [C₅₅H₇₈N₄NdO₂P] (1002.47 g/mol): C 65.90, H 7.84, N 5.59; found C 65.84, H 7.81, N 5.33.

Synthesis of [Na(18-crown-6)(thf)₂][(DippForm)₂Y(OCp)₂(thf)] (3)

To a mixture of [(DippForm)₂YCl(thf)] (**A**) (400 mg, 0.43 mmol, 1.00 eq.) and [Na(OCp)(dioxane)_{0.3}] (95 mg, 0.86 mmol, 2.00 eq.), thf (10 mL) was added. The resulting light-yellow suspension was stirred at room temperature for two hours before all volatiles were removed under vacuum. 18-crown-6 (114 mg, 0.43 mmol, 1.00 eq.) was added to the solid residue followed by thf (10 mL). The cloudy suspension was stirred at room temperature overnight. The precipitate was separated from the solution by cannula filtration. Upon addition of n-hexane, the product precipitated from the thf solution as a colourless powder (343 mg, 55% crude yield). Because the powder slowly decomposed when it was dried under vacuum, an aliquot (150 mg) was redissolved in thf and layered with n-hexane for further purification. Colourless crystals suitable for single crystal X-ray diffraction were obtained within days. ¹H NMR (500.3 MHz, thf-d₈): δ [ppm] = 1.08 (d, ³J_{H-H} = 6.8 Hz, 48H, CHMe₂), 1.77 (m, OCH₂CH₂ (thf)), 3.43 (m, fluxional, 4H, CHMe₂), 3.62 (m, overlapping, OCH₂ (thf)), 3.62 (m, overlapping, 24H, OCH₂CH₂O (18-crown-6)), 3.85 (m, fluxional, 4H, CHMe₂), 6.85 (m, fluxional, 12H, aromatic H), 7.81 (d, ³J_{H-γ} = 3.0 Hz, 2H, NCHN). VT ¹H NMR (400.2 MHz, thf-d₈, 333K): δ [ppm] = 1.09 (d, ³J_{H-H} = 6.7 Hz, 24H, CHMe₂), 1.12 (d, ³J_{H-H} = 6.7 Hz, 24H, CHMe₂), 1.77 (m, OCH₂CH₂ (thf)), 3.63 (m, overlapping, 8H, CHMe₂), 3.63 (m, overlapping, OCH₂ (thf)), 3.63 (m, overlapping, 24H, OCH₂CH₂O (18-crown-6)), 6.80 (t, ³J_{H-H} = 7.6 Hz, 4H, p-CH), 6.90 (d, ³J_{H-H} = 7.6 Hz, 8H, m-CH), 7.82 (d, ³J_{H-γ} = 3.1 Hz, 2H, NCHN). ¹³C{¹H} NMR (125.8 MHz, thf-d₈): δ [ppm] = 24.5 (brr, fluxional, CHMe₂), 26.6 (OCH₂CH₂ (THF)), 28.5 (br, fluxional, CHMe₂), 68.4 (OCH₂ (thf)), 70.9 (OCH₂CH₂O (18-crown-6)), 123.5 (br, fluxional, aromatic C), 160.4 (dd, ¹J_{C-P} = 18.0 Hz, ²J_{C-γ} = 3.7 Hz, OCp), 170.4 (d, ²J_{C-γ} = 3.0 Hz, NCHN). ³¹P{¹H} NMR (162.0 MHz, thf-d₈): δ [ppm] = −368.7. ⁸⁹Y{¹H} INEPT NMR (19.6 MHz, thf-d₈): δ [ppm] = 147.3 ppm. ¹H-⁸⁹Y HMQC NMR ((400.2 MHz / 19.6 MHz), thf-d₈): δ [ppm] = 7.81 / 147.3. IR (Nujol, cm^{−1}): 1799 (w), 1771 (w, OCp), 1600 (b), 1463

(s), 1377 (s), 1300 (w), 1260 (w), 1238 (w), 1152 (w), 1093 (m), 1020 (w), 944 (w), 800 (w), 722 (w). Elemental analysis calcd (%) for [C₇₆H₁₁₈N₄NaO₁₁P₂Y] (1437.64 g/mol): No satisfactory results could be obtained.

Synthesis of [Na(18-crown-6)(thf)₂][(DippForm)₂Nd(OCp)₂(thf)] (4)

To a mixture of [(DippForm)₂NdCl(thf)] (**A**) (210 mg, 0.21 mmol, 1.00 eq.) and [Na(OCp)(dioxane)_{0.3}] (47 mg, 0.43 mmol, 2.05 eq.), thf (10 mL) was added. The resulting light-yellow suspension was stirred at room temperature for two hours before all volatiles were removed under vacuum. 18-crown-6 (57 mg, 0.21 mmol, 1.00 eq.) was added to the solid residue followed by thf (10 mL). The cloudy suspension was stirred at room temperature overnight and subsequently filtered. The thf solution was concentrated and layered with n-hexane, which ultimately led to the formation of colorless (light bluish) crystals, which partially decompose over time. The mother liquor was removed via decantation and the crystalline residue was shortly dried under vacuum. Yield: 180 mg (58 %). Fresh samples can be crystallized from crude product. ¹H NMR (400.2 MHz, thf-d₈): δ [ppm] = −2.86 (bs), −1.40 (bs), 0.90 (s), 4.16 (bs, crown, thf), 5.72 (bs), 7.66 (bs), 9.30 (bs), 12.93 (bs), 21.11 (bs). Due to the paramagnetic nature of **4**, only broad and unstructured resonances were observed. ³¹P{¹H}NMR (162.0 MHz, thf-d₈): δ [ppm] = −289.7. IR (Nujol, cm^{−1}): 1702 (s), 1683 (s, OCp), 1591 (w), 1525 (s), 1351 (m), 1317 (m), 1284 (m), 1247 (m), 1191 (m), 1109 (s), 1054 (w), 964 (m), 937 (w), 844 (m), 800 (w), 772 (w), 756 (w), 722 (w). Elemental analysis calcd (%) for [C₇₆H₁₁₈N₄NaN₂O₁₁P₂] (1492.98 g/mol): No satisfactory results could be obtained.

Synthesis of [(DippForm)₂Nd(μ²-OCp)]₂ (5)

[(DippForm)₂Nd(OCp)(thf)] (**2**) (59 mg, 0.058 mmol, 1.00 eq.) and B(C₆F₅)₃ (30 mg, 0.058 mmol, 1.00 eq.) were added to an NMR or Schlenk tube and dissolved in benzene (1–2 mL). The pale blueish mixture was shaken until a clear solution was obtained and left standing for at two days. Light blue block-like crystals were obtained and separated from the mother liquor by decantation. The crystals were quickly washed with small amounts of benzene and dried under vacuum. Yield: 42 mg (78 %, single crystals). ¹H NMR (400.2 MHz, thf-d₈): δ [ppm] = −1.09 (bs), 1.19 (bs), 3.40 (bs), 7.10 (bs), 8.13 (bs), 29.14 (s). Due to the paramagnetic nature of **5**, only broad and unstructured resonances were observed. ³¹P{¹H} NMR (162.0 MHz, thf-d₈): δ [ppm] = −278.1. IR (Nujol, cm^{−1}): 1748 (m, OCp), 1363 (w), 1260 (m), 1156 (m), 1094 (br), 1021 (br), 800 (s), 720 (w). Elemental analysis calcd (%) for [C₁₀₂H₁₄₀N₈Nd₂O₂P₂] (1860.73 g/mol): C 65.84, H 7.58, N 6.02; found 65.42, H 7.27, N 5.97.

Synthesis of [(DippForm)Sm(18-crown-6)(thf)][DippForm] (6)

[(DippForm)₂Sm(thf)₂] (50 mg, 0.04 mmol, 1.00 eq.) and 18-crown-6 (13 mg, 0.04 mmol, 1.00 eq.) were dissolved in thf (0.6 mL) in an J. Young NMR tube and shaken until a clear green solution was obtained. The mixture was concentrated to approximately 0.2 mL and layered with n-hexane. Dark green crystals were obtained within a few days, separated from the mother liquor by decantation and dried under vacuum. Yield: 35 mg (60 %, single crystals). ¹H NMR (400.2 MHz, thf-d₈): δ

[ppm] = -9.58, 1.47, 3.62, 3.66, 5.32, 6.79, 7.43. Due to the paramagnetic nature of **6**, only broad and unstructured resonances were observed. IR (Nujol, cm^{-1}): 2723 (w), 1591 (w), 1541 (m), 1342 (w), 1303 (m), 1236 (w), 1180 (w), 1154 (vw), 1085 (m), 1038 (w), 961 (w), 920 (vw), 896 (vw), 837 (vw), 777 (vw), 767 (vw), 757 (w), 721 (w). Elemental analysis calcd (%) for $[\text{C}_{66}\text{H}_{102}\text{N}_4\text{O}_7\text{Sm}]$ (1213.92 g/mol): C 65.30, H 8.47, N 4.62; found 64.76, H 8.44, N 4.39.

Synthesis of [(DippForm)Sm(OCP)(18-crown-6)] (7**)**
 $[(\text{DippForm})_2\text{Sm}(\text{thf})_2]$ (100 mg, 0.10 mmol, 1.00 eq.) and 18-crown-6 (26 mg, 0.10 mmol, 1.00 eq.) were dissolved in thf (2 mL) in an JYoung tube and stirred until a clear green solution was obtained (~ 1–2 hours). Subsequently, a solution of $[\text{Na}(\text{OCP})(\text{dioxane})_{0.3}]$ (11 mg, 0.10 mmol, 1.00 eq.) in thf (1 mL) was added to the reaction mixture, which was stirred for another 4 hours. The clear dark green solution was layered with n-hexane (25 mL) and left standing until dark green crystals formed (4–7 days). The crystals were isolated by decantation from the mother liquor and dried under vacuum. Yield: 42 mg (50 %, single crystals). Note: After prolonged periods, the formation of colorless block-like crystals is also observed, which were found to be the oxidized species $[\text{Na}(18\text{-crown-6})(\text{thf})_2][(\text{DippForm})_2\text{Sm}(\text{OCP})_2(\text{thf})]$ (**7b**, See crystallographic section for the structure). ^1H NMR (400.2 MHz, C_6D_6): δ [ppm] = -9.16 (bs, 2H, NCHN), 0.33 (bs, 12H, CH_3), 3.09 (bs, overlapping, 16H, CH_3 and $\text{CH}(\text{CH}_3)_2$), 4.91 (d, $^3J_{\text{H-H}} = 7.2$ Hz, 4H, m-CH), 6.29 (t, $^3J_{\text{H-H}} = 7.2$ Hz, 2H, p-CH), 6.56 (bs, 12H, CH_2), 8.51 (bs, 12H, CH_2). $^{13}\text{C}\{^1\text{H}\}$ NMR (125.8 MHz, C_6D_6): δ [ppm] = 22.9, 24.5, 35.6, 114.9, 115.8, 120.6, 124.5, 129.5. $^{31}\text{P}\{^1\text{H}\}$ NMR (162.0 MHz, C_6D_6): δ [ppm] = -391.7. IR (Nujol, cm^{-1}): 1758 (m, OCP), 1666 (w), 1592 (vw), 1526 (m), 1326 (w), 1295 (m), 1258 (w), 1183 (w), 1099 (m), 1079 (m), 995 (vw), 965 (w), 876 (vw), 838 (w), 802 (w), 763 (w), 721 (w). Elemental analysis calcd (%) for $[\text{C}_{38}\text{H}_{59}\text{N}_2\text{O}_7\text{Sm}]$ (837.23 g/mol): C 54.52, H 7.10, N 3.35; found 53.92, H 7.22, N 3.21.

Synthesis of [(2,2,2-crypt)Sm(OCP)] (8**)**
 $[(\text{DippForm})_2\text{Sm}(\text{thf})_2]$ (45 mg, 0.04 mmol, 1.00 eq.) and 2,2,2-crypt (16 mg, 0.04 mmol, 1.00 eq.) were dissolved in thf (0.6 mL) in an J. Young NMR tube and shaken until a clear red solution was obtained. The mixture was concentrated to approximately 0.2 mL and left standing overnight. Large dark-red crystals formed which were separated from the mother liquor by decantation and subsequently washed with thf (2 \times 0.5 mL) and dried under vacuum. Yield: 40 mg (80 %, single crystals). ^1H NMR (400.2 MHz, thf-d_8): δ [ppm] = -9.95, -2.50, -2.39, -1.80, -1.41, 0.00, 0.40, 0.60, 1.52, 2.92, 4.41, 6.12, 7.31, 8.30, 8.78, 11.41, 11.43. Due to the paramagnetic nature of **8**, only broad and unstructured resonances were observed. IR (Nujol, cm^{-1}): 1592 (w), 1377 (w), 1311 (w), 1342 (w), 1259 (w), 1235 (w), 1180 (w), 1092 (w), 1063 (w), 1018 (w), 802 (w). Elemental analysis calcd (%) for $[\text{C}_{68}\text{H}_{106}\text{N}_6\text{O}_6\text{Sm}]$ (1253.99 g/mol): C 65.13, H 8.52, N 6.70; found C 65.01, H 8.49, N 6.41.

Synthesis of [(2,2,2-crypt)Sm(OCP)] (9**)**
 A mixture of $[(\text{DippForm})_2\text{Sm}(\text{thf})_2]$ (100 mg, 0.10 mmol, 1.00 eq.) and 2,2,2-crypt (37 mg, 0.10 mmol, 1.00 eq.) was dissolved in thf (2 mL) inside the glovebox. The solution was left standing at room temperature for 2 hours and during this

period, a colour change of the solution from green to red was observed. $[\text{Na}(\text{OCP})(\text{dioxane})_{0.3}]$ (22 mg, 0.20 mmol, 2.00 eq.) was added to the solution as a solid, and red crystals suitable for single crystal X-ray diffraction rapidly formed. Yield: 30 mg (47 %, single crystals). ^1H NMR (500.3 MHz, $\text{d}_5\text{-pyridine}$): δ [ppm] = 1.46 (s, 12H, NCH_2), 3.26 (s, 12H, $\text{OCH}_2\text{CH}_2\text{O}$), 3.58 (s, 12H, $\text{NCH}_2\text{CH}_2\text{O}$). $^{13}\text{C}\{^1\text{H}\}$ NMR (125.8 MHz, $\text{d}_5\text{-pyridine}$): δ [ppm] = 92.4 (NCH_2), 99.4 ($\text{NCH}_2\text{CH}_2\text{O}$), 99.6 ($\text{OCH}_2\text{CH}_2\text{O}$), 183.9 (d, $^1J_{\text{C-P}} = 48.4$ Hz, OCP). $^{31}\text{P}\{^1\text{H}\}$ NMR (162.0 MHz, $\text{d}_5\text{-pyridine}$): δ [ppm] = -374.0 (s). IR (Nujol, cm^{-1}): 1782 (w), 1763 (PCO), 1749 (PCO), 1623 (b), 1463 (s), 1377 (s), 1351 (w), 1302 (w), 1261 (w), 1125 (m), 1090 (m), 1066 (m), 1030 (b), 957 (w), 800 (w), 722 (w), 668 (w). Elemental analysis calcd (%) for $[\text{C}_{20}\text{H}_{36}\text{N}_2\text{O}_8\text{P}_2\text{Sm}]$ (644.82 g/mol): C 37.25, H 5.63, N 4.34; found C 37.39, H 5.62, N 4.30.

Analytical techniques

Single crystal X-ray structure determination: Single-crystal X-ray diffraction data were collected using an Oxford Diffraction Supernova dual-source diffractometer equipped with a 135 mm Atlas CCD area detector. Crystals were selected under Paratone-N oil, mounted on micromount loops and quenched using an Oxford Cryosystems open flow N_2 cooling device.⁴⁰ Data were collected at 150 K using mirror monochromated Cu $\text{K}\alpha$ radiation ($\lambda = 1.5418$ Å; Oxford Diffraction Supernova). Data collected on the Oxford Diffraction Supernova diffractometer were processed using the CrysAlisPro package, including unit cell parameter refinement and inter-frame scaling (which was carried out using SCALE3 ABSPACK within CrysAlisPro).⁴¹ Equivalent reflections were merged and diffraction patterns processed with the CrysAlisPro suite. Structures were subsequently solved using direct methods and refined on F^2 using the ShelXL 2013 package and ShelXle.^{42, 43}

Crystallographic data for the structures reported in this paper have been deposited with the Cambridge Crystallographic Data Centre as a supplementary publication No. 1857886-1857895. Copies of the data can be obtained free of charge on application to CCDC, 12 Union Road, Cambridge CB21EZ, UK (fax: (+44)1223-336-033; email: deposit@ccdc.cam.ac.uk). NMR samples were prepared inside an inert atmosphere glovebox in NMR tubes fitted with a gas-tight valve. ^1H , ^{11}B , $^{13}\text{C}\{^1\text{H}\}$, ^{19}F , and $^{31}\text{P}\{^1\text{H}\}$ NMR spectra were recorded on the following NMR instruments with appropriate resonance frequencies: a) Bruker Avance III HD nanobay NMR equipped with a 9.4 T magnet (^1H 400.2 MHz, ^{11}B 128.4 MHz, ^{13}C 100.6 MHz, ^{19}F 376.5 MHz, ^{31}P 162.0 MHz), b) Bruker Avance III NMR equipped with a 11.75 T magnet (^1H 499.9 MHz, ^{11}B 160.4 MHz, ^{13}C 125.7 MHz, ^{19}F 470.4 MHz, ^{31}P 202.4 MHz), c) Bruker Avance NMR equipped with a 11.75 T magnet and a ^{13}C detect cryoprobe (^1H 500.3 MHz, ^{13}C 125.8 MHz). $^{89}\text{Y}\{^1\text{H}\}$ INEPT and $^1\text{H}\{^{89}\text{Y}\}$ HMQC NMR spectra were recorded at 19.6 MHz and (400.2 MHz / 19.6 MHz), respectively, on the Bruker Avance III HD nanobay NMR. ^1H and $^{13}\text{C}\{^1\text{H}\}$ NMR spectra are reported relative to TMS and referenced to the most downfield residual solvent resonance where possible. $^{31}\text{P}\{^1\text{H}\}$ NMR spectra were

externally referenced to an 85% solution of H_3PO_4 in H_2O ($\delta = 0$ ppm). $^{89}\text{Y}\{^1\text{H}\}$ NMR spectra were externally referenced to a 1M solution of $\text{Y}(\text{NO}_3)_3(\text{H}_2\text{O})_6$ in D_2O .

IR spectra were obtained on a Bruker Tensor 37 as Nujol mulls. Elemental analyses were carried out by Elemental Microanalyses Ltd. (Devon, U. K.). Samples (approx. 10 mg) were submitted in sealed Pyrex ampoules.

Acknowledgements

The authors declare no competing interests. S. B. gratefully acknowledges a research fellowship provided by the DFG [BE 6401/1-1] (Project number 380155090).

References

1. G. Becker, W. Schwarz, N. Seidler and M. Westerhausen, *Z. Anorg. Allg. Chem.*, 1992, **612**, 72-82.
2. F. F. Puschmann, D. Stein, D. Heift, C. Hendriksen, Z. A. Gal, H. F. Grützmacher and H. Grützmacher, *Angew. Chem. Int. Ed.*, 2011, **50**, 8420-8423.
3. I. Krummenacher and C. C. Cummins, *Polyhedron*, 2012, **32**, 10-13.
4. A. R. Jupp and J. M. Goicoechea, *Angew. Chem. Int. Ed.*, 2013, **52**, 10064-10067.
5. D. Heift, Z. Benko and H. Grützmacher, *Dalton Trans.*, 2014, **43**, 831-840.
6. G. Hierlmeier, A. Hinz, R. Wolf and J. M. Goicoechea, *Angew. Chem. Int. Ed.*, 2018, **57**, 431-436.
7. D. Heift, Z. Benko, H. Grützmacher, A. R. Jupp and J. M. Goicoechea, *Chem. Sci.*, 2015, **6**, 4017-4024.
8. A. R. Jupp and J. M. Goicoechea, *J. Am. Chem. Soc.*, 2013, **135**, 19131-19134.
9. T. P. Robinson, M. J. Cowley, D. Scheschewitz and J. M. Goicoechea, *Angew. Chem. Int. Ed.*, 2015, **54**, 683-686.
10. T. P. Robinson and J. M. Goicoechea, *Chem. Eur. J.*, 2015, **21**, 5727-5731.
11. D. Heift, Z. Benkő and H. Grützmacher, *Angew. Chem. Int. Ed.*, 2014, **53**, 6757-6761.
12. A. Hinz, R. Labbow, C. Rennick, A. Schulz and J. M. Goicoechea, *Angew. Chem. Int. Ed.*, 2017, **56**, 3911-3915.
13. A. R. Jupp, M. B. Geeson, J. E. McGrady and J. M. Goicoechea, *Eur. J. Inorg. Chem.*, 2016, **2016**, 639-648.
14. A. Hinz and J. M. Goicoechea, *Angew. Chem. Int. Ed.*, 2016, **55**, 8536-8541.
15. A. Hinz and J. M. Goicoechea, *Angew. Chem. Int. Ed.*, 2016, **55**, 15515-15519.
16. S. Alidori, D. Heift, G. Santiso-Quinones, Z. Benkő, H. Grützmacher, M. Caporali, L. Gonsalvi, A. Rossin and M. Peruzzini, *Chem. Eur. J.*, 2012, **18**, 14805-14811.
17. C. Camp, N. Settineri, J. Lefevre, A. R. Jupp, J. M. Goicoechea, L. Maron and J. Arnold, *Chem. Sci.*, 2015, **6**, 6379-6384.
18. C. J. Hoerger, F. W. Heinemann, E. Louyriac, L. Maron, H. Grützmacher and K. Meyer, *Organometallics*, 2017, **36**, 4351-4354.
19. L. N. Grant, B. Pinter, B. C. Manor, H. Grützmacher and D. J. Mindiola, *Angew. Chem. Int. Ed.*, 2018, **57**, 1049-1052.
20. R. J. Gilliard, D. Heift, Z. Benko, J. M. Keiser, A. L. Rheingold, H. Grützmacher and J. D. Protasiewicz, *Dalton Trans.*, 2018, **47**, 666-669.
21. M. Westerhausen, S. Schneiderbauer, H. Piotrowski, M. Suter and H. Nöth, *J. Organomet. Chem.*, 2002, **643-644**, 189-193.
22. D. W. N. Wilson, A. Hinz and J. M. Goicoechea, *Angew. Chem. Int. Ed.*, 2018, **57**, 2188-2193.
23. G. B. Deacon, P. C. Junk, J. Wang and D. Werner, *Inorg. Chem.*, 2014, **53**, 12553-12563.
24. G. B. Deacon, P. C. Junk, L. K. Macreadie and D. Werner, *Eur. J. Inorg. Chem.*, 2014, **2014**, 5240-5250.
25. F. T. Edelmann, *Chem. Soc. Rev.*, 2012, **41**, 7657-7672.
26. M. L. Cole and P. C. Junk, *Chem. Commun.*, 2005, DOI: 10.1039/b501447f, 2695-2697.
27. C. Schoo, S. Bestgen, M. Schmidt, S. N. Konchenko, M. Scheer and P. W. Roesky, *Chem. Commun.*, 2016, **52**, 13217-13220.
28. G. B. Deacon, M. E. Hossain, P. C. Junk and M. Salehisaki, *Coord. Chem. Rev.*, 2017, **340**, 247-265.
29. Y. Z. Ma, S. Bestgen, M. T. Gamer, S. N. Konchenko and P. W. Roesky, *Angew. Chem. Int. Ed.*, 2017, **56**, 13249-13252.
30. C. Schoo, S. Bestgen, R. Koppe, S. N. Konchenko and P. W. Roesky, *Chem. Commun.*, 2018, **54**, 4770-4773.
31. M. L. Cole, G. B. Deacon, C. M. Forsyth, P. C. Junk, K. Konstas, J. Wang, H. Bittig and D. Werner, *Chem. Eur. J.*, 2013, **19**, 1410-1420.
32. M. L. Cole, G. B. Deacon, C. M. Forsyth, P. C. Junk, K. Konstas and J. Wang, *Chem. Eur. J.*, 2007, **13**, 8092-8110.
33. M. L. Cole and P. C. Junk, *J. Organomet. Chem.*, 2003, **666**, 55-62.
34. S. O. Grim and S. A. Sangokoya, *J. Chem. Soc., Chem. Commun.*, 1984, DOI: DOI 10.1039/c39840001599, 1599-1600.
35. Y. K. Gun'ko, P. B. Hitchcock and M. F. Lappert, *Chem. Commun.*, 1998, DOI: 10.1039/A805544K, 1843-1844.
36. D. N. Huh, C. M. Kotyk, M. Gembicky, A. L. Rheingold, J. W. Ziller and W. J. Evans, *Chem. Commun.*, 2017, **53**, 8664-8666.
37. A. G. Massey and A. J. Park, *J. Organomet. Chem.*, 1964, **2**, 245-250.
38. K. Hirano, S. Urban, C. Wang and F. Glorius, *Org. Lett.*, 2009, **11**, 1019-1022.
39. P. L. Watson, T. H. Tulip and I. Williams, *Organometallics*, 1990, **9**, 1999-2009.
40. J. Cosier and A. M. Glazer, *J. Appl. Crystallogr.*, 1986, **19**, 105-107.
41. CrysAlisPro, Agilent Technologies, Version 1.171.35.8.
42. G. M. Sheldrick, 2013, SHELXS-2013.
43. C. B. Hubschle, G. M. Sheldrick and B. Dittrich, *J. Appl. Crystallogr.*, 2011, **44**, 1281-1284.

TOC

The reactivity and coordination behaviour of the heavier cyanate analogue OCP^- towards three representative rare-earth elements Y, Nd and Sm was investigated. Mono- and bis-phosphaethynolate complexes in different oxidation states were prepared, leading to novel coordination modes of OCP^- and ionic intermediates of Sm(II) in the presence of 18-crown-6 or 2,2,2-crypt.

